RSC Advances

PAPER

View Article Online
View Journal | View Issue



Cite this: *RSC Adv.*, 2026, **16**, 15187

# Molecular mechanism of silver nanoparticles inhibiting primary root growth of *Oryza sativa* L

Jiajia Yang, Ruihua Chen, Huan Zhang, Ruonan Wang and Zhifeng Zhang *

Elucidating the phytotoxicity of silver nanoparticles (AgNPs) at the primary tissue level is essential for a comprehensive assessment of their ecotoxicological risks. This study systematically investigated the phytotoxic mechanisms of polyethyleneimine-coated silver nanoparticles (AgNPs@PEI) on plant primary roots using rice (*Oryza sativa* L.) primary roots as an experimental model through integrated physiological, transcriptomic, and metabolomic analyses. Exposure to AgNPs@PEI induced concentration-dependent growth inhibition, with a 10 mg $L^{-1}$ treatment causing a 44% reduction in root length, a 50% decrease in biomass, and a 28.3% shortening of the root meristematic zone, accompanied by abnormal root hair development and cap detachment. Physiological assessments revealed significant disturbances in root vitality and antioxidant enzyme activities (SOD, POD, and CAT). Transcriptomic profiling identified significant downregulation (fold change > 2) of genes involved in nine key metabolic pathways, most notably phenylpropanoid biosynthesis, aromatic amino acid (phenylalanine/tyrosine/tryptophan) biosynthesis, and glutathione metabolism. Metabolomic analysis revealed concomitant disruptions in seven essential pathways, particularly those involved in unsaturated fatty acid biosynthesis. These transcriptomic and metabolic alterations collectively impaired cell wall lignification through suppression of the phenylpropanoid pathway and compromised membrane integrity *via* dysregulation of fatty acid metabolism. This research elucidates the phytotoxic effects of AgNPs from a primary plant tissue perspective, providing novel evidence for understanding nanomaterial–plant interactions at the tissue level.

Received 23rd July 2025
Accepted 26th February 2026

DOI: 10.1039/d5ra05319f

rsc.li/rsc-advances



## 1 Introduction

Silver nanoparticles (AgNPs) have gained extensive applications across diverse industries, including electronics, textiles, medical devices, and food packaging, owing to their exceptional electrical conductivity, photochemical properties, and antimicrobial efficacy. In agricultural production, AgNPs have emerged as promising alternatives to conventional antimicrobial agents (*e.g.*, antibiotics and disinfectants) due to their broad-spectrum antibacterial activity.[1] However, a comprehensive understanding of their biological effects remains a prerequisite for agricultural application.

AgNPs not only impair seed germination and plant growth but also trigger excessive reactive oxygen species (ROS) accumulation in plant cells, disrupting normal physiological and metabolic processes.[2] As the primary interface between plants and their environment, the root system plays a crucial role in mediating responses to environmental stressors. Current studies on the effects of AgNPs on root morphology and physiology have consistently shown that AgNP exposure significantly impairs root system development. These adverse effects include inhibited root elongation, suppressed root formation, and reduced overall root biomass.[3,4] For instance, Yin *et al.* demonstrated that AgNP exposure suppresses plant root growth, primarily by disrupting cell division and elongation in root tips.[5] Similarly, Mirzajani *et al.* observed that AgNP exposure frequently leads to significant biomass reduction in plants. This phenomenon primarily results from root system impairment, which subsequently restricts water and nutrient uptake capacity, ultimately compromising overall plant growth and physiological performance.[6] Some studies also demonstrated that they exhibit dose-dependent regulation of root development, as exemplified in *Arabidopsis thaliana*, where low concentrations (typically < 50 mg $L^{-1}$) stimulate root elongation while higher concentrations exert inhibitory effects through modulation of cell cycle dynamics and reactive oxygen species (ROS) accumulation.[7] This response pattern has been documented not only in model plants such as *Arabidopsis thaliana* and *Oryza sativa*,[8,9] but also in agriculturally significant species including *Triticum aestivum*, *Vicia faba*, *Raphanus sativus*, and *Solanum tuberosum*.[10,11] The phytotoxic effects of AgNPs on plant roots are mediated through multiple interconnected mechanisms. Primarily, the physical interaction between AgNPs and root tissues can cause direct mechanical damage, thereby impairing root growth and development.[12] At the cellular level, AgNPs induce excessive generation of reactive oxygen species (ROS), resulting in oxidative stress that damages critical cellular components including membrane lipids, functional proteins, and genetic

*School of Life Science, Shanxi Normal University, Taiyuan, 030031, China. E-mail: zzfsx2012@126.com; Fax: +(86)-0351 2051196*

material.[13,14] Furthermore, the dissolution of AgNPs releases bioactive silver ions ($Ag^+$), which disrupt cellular homeostasis by binding to sulfhydryl groups in proteins and interacting with nucleic acids, ultimately interfering with enzymatic activities and genetic processes.[13] However, more comprehensive evidence at the molecular level is required to elucidate the precise mechanisms underlying these observed effects.[15]

The primary meristem, as the initial structural foundation for plant morphogenesis, plays a pivotal role in determining both organogenesis and subsequent growth and developmental processes.[16] The primary root, developing directly from the radicle during seed germination, constitutes the plant's first part of the root system that ensures seedling establishment through water and nutrient acquisition, physical anchorage, and environmental adaptation.[17] The primary root exhibits a well-defined longitudinal organization comprising three distinct functional zones: meristematic, elongation, and maturation.[18] The primary root growth is largely established by the division of meristem cells at the meristematic zone, and subsequent elongation of the cells at the elongation zone and differentiation of the cells at the maturation zone in the root tip.[19,20] With its straightforward anatomical architecture (primary tissues only) and limited developmental complexity (no secondary growth), the primary root serves as an ideal experimental model for elucidating the key physiological and molecular processes underlying root responses to diverse environmental challenges, such as heavy metal toxicity, osmotic stress, and organic pollutant exposure, in complex soil-plant systems.[21,22]

Rice (*Oryza sativa* L), an essential food crop, serves as a primary staple for over half of the global population.[23,24] Moreover, rice represents an ideal monocot model for investigating nanomaterial–plant interactions, particularly due to its suitability for controlled hydroponic experiments. Accordingly, the present study adopted the primary root of rice as a model system to systematically examine the biological effects of AgNPs from the perspective of plant primary tissues.

By integrating multi-scale analytical methods, we first observed the macroscopic morphological and microstructural changes in rice primary roots under AgNPs exposure and quantitatively assessed variations in growth parameters such as root length and biomass. We further analyzed the changes in the activities of key enzymes within the primary roots. Concurrently, high-throughput genomics and metabolomics technologies were employed to elucidate the changes in gene expression levels and metabolic pathways in rice primary roots responding to AgNPs stress. This study not only reveals the physiological and molecular mechanisms by which AgNPs affect the development of plant primary tissues but also provides a theoretical basis for a deeper understanding of the phytotoxic effects of nanomaterials.

# 2 Materials and methods

## 2.1 Chemicals and reagents

Silver nitrate ($AgNO_3$, >99.5%) was obtained from Sinopharm Chemical Reagent Co., Ltd (Shanghai, China). Polyethyleneimine (PEI, MW 600 Da) was purchased from Aladdin Chemistry Co., Ltd (Shanghai, China). Sodium borohydride ($NaBH_4$) was acquired from Sigma-Aldrich (St. Louis, MO, USA). Ultrafiltration was performed using Amicon® Ultra-15 centrifugal filters (3 kDa MWCO, Merck Millipore, Germany). All other chemicals were of analytical grade. Deionized water (18.2 MΩ cm) was purified using a Millipore Milli-Q system (Burlington, MA, USA) for all experiments.

## 2.2 Synthesis and characterization of AgNPs

The AgNPs@PEI nanocomposite was synthesized according to our previously reported method.[25] Briefly, 10 mL of $AgNO_3$ solution (4.76 mM) was added into 200 mL of PEI solution (0.5 mg $mL^{-1}$) under vigorous magnetic stirring (800 rpm) at 25 °C. After stirring for 1 h, 20 μL of freshly prepared $NaBH_4$ solution (39.5 mM) was introduced as reducing agent, and the reaction proceeded for 3 h to ensure complete reduction of $Ag^+$ ions. The prepared AgNPs suspension was purified by centrifugal ultrafiltration (Amicon Ultra-15, 50 kDa, Millipore) to remove excess $Ag^+$, PEI and $NaBH_4$, respectively. The morphological characteristics of AgNPs@PEI were analyzed using transmission electron microscopy (TEM), while the surface chemical states were investigated by X-ray photoelectron spectroscopy (XPS). The measurements of zeta potential, hydrodynamic diameter, and silver ion release are provided in the SI.

## 2.3 Plant culture and treatment

Plump seeds of rice (*Oryza sativa* L. cv. Zhonghua 11) were surface-sterilized with 2% $H_2O_2$ for 30 min and thoroughly rinsed with distilled water. The seeds were germinated on seedling trays in darkness at 25 °C for 3 days, after which the temperature was increased to 30 °C for 24 h to promote radicle emergence. Uniformly germinated seeds were then transferred to hydroponic boxes containing 20% Hoagland nutrient solution (the chemical composition of the full-strength Hoagland nutrient solution is provided in Table S2; its pH is approximately 5.2). In accordance with current literature on the phytotoxicity of AgNPs,[26–29] the exposure concentration range was selected as 0–10 mg $L^{-1}$. AgNPs@PEI were added to the nutrient solutions at concentrations of 0, 0.1, 1.0, 5.0, and 10.0 mg $L^{-1}$. Seedlings were grown in a phytotron under a 16 h light/8 h dark photoperiod at 28 °C. The treatment without AgNPs@PEI served as the blank control, and each concentration was tested in three biological replicates. Following 72 h of exposure, the effects of AgNPs@PEI on rice primary root growth were assessed. Considering the intrinsic phytological effects of silver nanoparticles, no control groups for silver ions or free coating PEI were established.

## 2.4 Morphological analysis

Primary root lengths were measured using a root scanner, and the acquired images were processed with Image Pro Plus software. Root morphology was compared between AgNPs@PEI-treated and control (CK) groups using a stereo light microscope (SLM). To examine the root cap structure and root hair density, approximately 2 cm of primary roots were excised from

3-days-old seedlings. The samples were fixed in 2.5% glutaraldehyde for 1 hour at room temperature, followed by three rinses with phosphate buffer to remove residual fixative. A graded ethanol series (30%, 50%, 70%, 80%, 95%, and 100%) was then used for dehydration, with each step lasting 15 min. After dehydration, the samples were freeze-dried to preserve fine surface morphology. Prior to SEM observation, the dried specimens were mounted on stubs and sputter-coated with a gold-palladium layer. Primary roots from 10 randomly selected 3-days-old rice seedlings under different treatments were rinsed with ultrapure water (18.2 MΩ cm resistivity, further purified from deionized water), stained with aceto-carmine solution for 5 min, then washed with 95% ethanol for 3 min, and rinsed three times with ultrapure water. The staining roots were observed under a microscope, and the length of the root apical meristem was measured using Image-Pro Plus software.[30]

### 2.5 Analysis of physiological parameters

**2.5.1 Primary root viability assay.** Cell viability was assessed using a modified Evans blue staining method.[31] Primary roots from each treatment were immersed in 0.25% (v/v) Evans blue solution for 15 min, followed thorough rinsing with ultrapure water. The stained roots were then incubated in *N*,*N*-dimethylformamide (1 : 10, w/v) at room temperature for 2 h to extract the dye. Roots subjected to boiling water for 15–20 min before staining served as the positive control. After extraction, the samples were centrifuged at 8000 rpm for 4 min. The absorbance of Evans blue in the supernatant was measured at 600 nm. Relative cell viability (V) was calculated using the following formula:

$$V = [1 - (A/B] \times 100\%$$

where: $A$ is the absorbance of the extraction solution from the treated root tips; $B$ is the absorbance of the extraction solution from the killed root tips.

**2.5.2 Determination of lipid peroxidation and hydrogen peroxide levels.** Lipid peroxidation was assessed by measuring malondialdehyde (MDA) content according to the thiobarbituric acid (TBA) method.[32] Hydrogen peroxide ($H_2O_2$) concentration was quantified following the protocol of Jena and Choudhuri.[33] Detailed experimental procedures are provided in the SI.

**2.5.3 Determination of antioxidant enzyme activities.** Fresh primary roots were homogenized in ice-cold 50 mM phosphate buffer (pH 7.8) using a pre-chilled mortar and pestle. The homogenate was centrifuged at 8000×*g* for 10 min at 4 °C, and the resulting supernatant was collected for enzyme activity assays. Activities of superoxide dismutase (SOD), peroxidase (POD), and catalase (CAT) were determined using commercial assay kits (Sangon Biotech, Shanghai, China; SOD: Cat. No. D799593, POD: D799591, CAT: D799597). Assays were performed according to the manufacturer's instructions, based on spectrophotometric detection at 560 nm (SOD), 470 nm (POD), and 240 nm (CAT), respectively. Enzyme activities were calculated from the corresponding standard curves and expressed as units per milligram of protein (U $mg^{-1}$ protein).

### 2.6 Transcriptome analysis

The rice seedlings were separately treated with 0, 5.0, 10.0 mg $L^{-1}$ AgNPs@PEI for 3 days. The primary roots were sampled, washed with ultrapure water three times, immediately put into a centrifuge tube, and frozen with liquid nitrogen for 15 minutes. Total RNA was extracted by TRIzol reagent (Invitrogen, Carlsbad, USA). Total amounts and integrity of RNA were assessed using the RNA NanDrop 2000 Assay Kit of the Bioanalyzer 2100 system (Agilent Technologies, CA, USA). The cDNA library was sequenced on the Illumina sequencing platform by Personal Biotechnology Co., Ltd (Shanghai, China). The differentially expressed genes (DEGs) of the primary root were identified by the DEGseq2 package. The Gene Ontology (GO) functional enrichment analysis and Kyoto Encyclopedia of Genomes (KEGG) pathway enrichment analysis of DEGs were performed using GOseq (1.10.0) and KOBAS (v2.0.12) software. Detailed experimental procedures are provided in the SI.

### 2.7 Metabolite profiling analysis

Approximately 0.2 g (±1%) of the primary roots of AgNPs@PEI treated with 0, 5.0, and 10.0 mg $L^{-1}$ AgNPs@PEI were rapidly frozen in liquid nitrogen for subsequent analysis. Sample preparation and data analysis for metabolomics analyses were performed using standard procedures at Personal Biotechnology Co., Ltd (Shanghai, China). LC-MS/MS analyses were performed using a UHPLC system (Agilent 1290 Infinity LC) coupled with an AB Triple TOF 6600 mass spectrometer (AB SCIEX)20. We performed Principal Component Analysis (PCA) and Partial Least Squares Discriminant Analysis (PLS-DA) to generate values of the Variable Importance in the Projection (VIP). The metabolites with VIP > 1 and *P*-value < 0.05 were considered to be differentially expressed metabolites (DEMs). The DEMs were annotated using the KEGG database (https://www.jp/kegg/) and HMDB database (https://www.hmdb.ca/). Detailed experimental procedures are provided in the SI.

### 2.8 Statistical analysis

All experimental results are presented as mean values ± standard deviation. Three replicates were performed in the plant growth experiments. Six independent biological replicates were conducted for untargeted metabolomics profiling. For transcriptomic analysis, three independent biological replicate samples were randomly selected from the six metabolome replicates of each treatment. Statistical significance was determined by one-way ANOVA with Duncan's multiple range test ($p < 0.05$). Data analysis was performed using SigmaPlot software (v14.0, Systat Software). Additional analyses included heat map generation using Microsoft Excel (v15.32 for Mac) and pathway enrichment analysis using Metabolic Analysis Software (v4.0, https://www.genescloud.cn).

## 3 Results and discussion

### 3.1 Characteristics of AgNPs

The transmission electron microscopy (TEM) image of the synthesized AgNPs is presented in Fig. 1A, showing

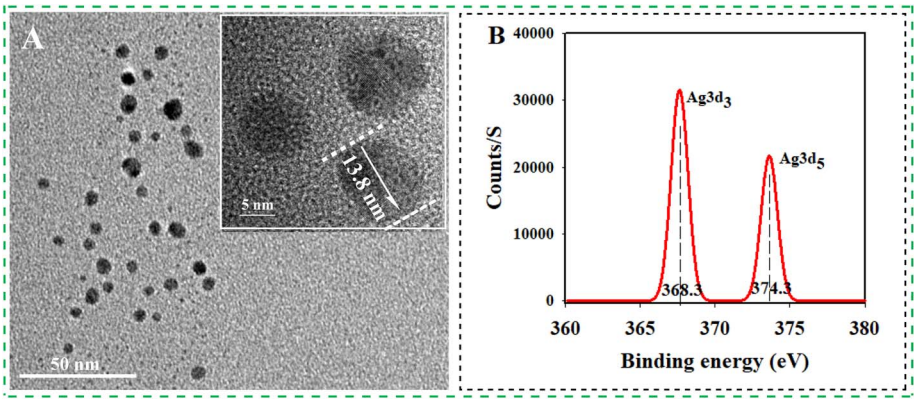


Fig. 1 (A) TEM image of AgNPs@PEI (B) XPS spectrum of AgNPs@PEI.

nanoparticles with an average size of approximately 35 ± 9 nm and a predominantly spherical morphology. The X-ray photoelectron spectroscopy (XPS) spectrum of AgNPs, as illustrated in Fig. 1B, exhibits two distinct peaks centered at binding energies of 368.3 eV and 374.3 eV, corresponding to Ag $3d_{5/2}$ and Ag $3d_{3/2}$, respectively. These binding energy values align well with those of metallic silver ($Ag^0$), providing strong evidence for the successful formation of AgNPs.[34] The surface zeta potential, dispersibility, and stability of AgNPs@PEI were evaluated in the medium used for rice primary root culture. As shown in Fig. S1A, the surface zeta potential of AgNPs@PEI in 20% Hoagland nutrient solution (pH 6.0) increased slightly from +13.2 mV in distilled water to +16.7 mV after 3 days, which may be attributed to the protonation of amino groups in PEI under acidic conditions, leading to enhanced positive surface charge density.[35] The dispersibility of AgNPs@PEI in the nutrient solution decreased slightly, as reflected by an increase in hydrodynamic diameter from 82.26 nm to 107.76 nm (Fig. S1B). UV-vis absorption spectra of AgNPs@PEI in the nutrient solution showed no significant changes compared to those in distilled water (Fig. S1C), indicating negligible oxidation or morphological alteration of AgNPs@PEI. The cumulative concentration of released $Ag^+$ from AgNPs@PEI reached 294.7 μg $L^{-1}$ after 3 days of incubation, corresponding to an $Ag^+$ release ratio of approximately 6.27% (Fig. S1D). These results suggest a slow $Ag^+$ release process in the nutrient medium.

### 3.2 Effect of AgNPs on the morphology of rice primary roots

**3.2.1 Effect on the biomass of rice primary roots.** The root system is a sensitive organ of plants subjected to external stimuli. Some studies have reported that certain engineered nanomaterials can stimulate early root growth.[36] However, our results indicated that AgNPs inhibited the primary root growth in a concentration-dependent manner, with increasing concentrations of AgNPs from 0.1 to 10 mg $L^{-1}$ (Fig. S2, SI). Compared with CK, 10 mg $L^{-1}$ AgNPs resulted in a significant reduction in primary root length, with an average decrease of 1.07 ± 0.375 cm (Fig. S3A). This observation aligns with previous findings demonstrating that elevated concentrations of nanoceria inhibit root elongation in pea (*Pisum sativum*).[37] This suggests a general trend where higher concentrations of nanomaterials may inhibit primary root growth while altering root morphology.[38] As shown in Fig. S3B, dry biomass accumulation in rice primary roots showed no significant change after a 3-days exposure to AgNPs at concentrations ≤1.0 mg $L^{-1}$. However, at higher concentrations, biomass accumulation decreased progressively. This trend demonstrates that the sensitivity of primary roots to AgNPs-induced stress increases with treatment levels. Consistent with previous findings, the presence of nanoparticles in growth media significantly reduced both fresh and dry biomass of *Brassica nigra* plants in a concentration-dependent manner.[39] These growth reductions likely stem from nanoparticle uptake and subsequent intracellular accumulation, leading to phytotoxic effects including: suppression of cell elongation and division, disruption of growth regulation, growth, and impairment of water and nutrient acquisition.[40]

**3.2.2 Effect on root hairs and root cap.** Microscopic analysis revealed that AgNPs exposure significantly impaired rice root hair development (Fig. 2A). The number of primary root hairs significantly decreased at AgNPs concentrations above 1.0 mg $L^{-1}$. SEM imaging further demonstrated distinct morphological alterations in root hair structure (Fig. 2C). It is well known that root hairs are the main site of plants for absorbing water and inorganic salts.[41] The inhibitory effect of AgNPs on root hair development may contribute to the observed impairment of primary root growth. This finding aligns with previous reports by Zhang *et al.*, who demonstrated that nanoparticle accumulation on root surfaces can physically obstruct epidermal openings, thereby disrupting water transport mechanisms in both tomato and reed plants.[42] Intriguingly, our investigations uncovered that AgNPs trigger premature root cap abscission in rice primary roots. From Fig. 2B, it can be seen that control (CK) roots maintained intact root caps throughout the 3-days cultivation period. The concentration of AgNPs reaches 5.0 mg $L^{-1}$, and the root caps show obvious signs of detachment. SEM observations further confirmed this dose-dependent morphological alteration (Fig. 2D). The root cap, as a protective structure at the tip, plays an important role in protecting the apical meristem.[43] AgNPs-induced root cap

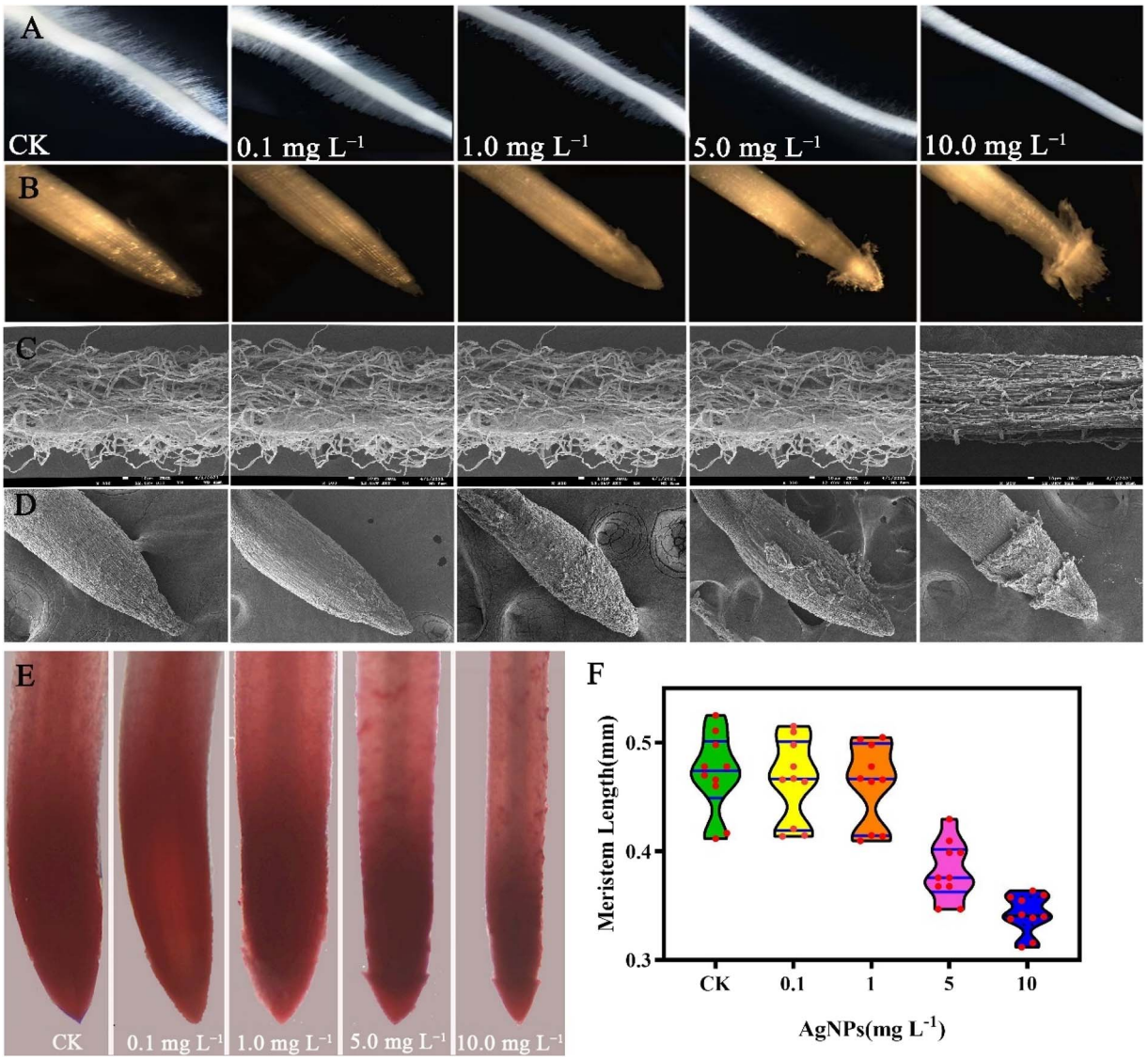


Fig. 2 Microscopic observation of root hairs (A) and root caps (B) of rice primary roots exposed to AgNPs@PEI SEM observation of root hairs (C) and root caps (D) of rice primary roots exposed to AgNPs@PEI Effect of AgNPs@PEI on images of acetocarimine-stained root meristems (E) and meristematic zone length (F).

detachment may consequently compromise meristematic zone integrity and disrupt normal root tip physiology.[44]

**3.2.3 Effects on the meristematic zone of root tips.** Plant root growth depends critically on the division of meristematic cells and the growth of elongation cells in the root tip.[45–47] The meristematic zone is the most active area for cell division of the root tip.[48] Acetic acid magenta staining revealed that AgNPs exposure reduces the meristematic zone length in primary root tips (Fig. 2E). Statistical evaluation demonstrated a 28.3% decrease in meristem length at 10 mg $L^{-1}$ AgNPs exposure (0.339 ± 0.029 mm) compared to controls (0.473 ± 0.035 mm) (Fig. 2F). The observed reduction in rice primary root length likely results from AgNPs-induced inhibition of cell proliferation in the meristematic zone.[49] This mechanism is consistent with previous findings on nanoparticle phytotoxicity, including Wang *et al.*'s demonstration of meristem cell vacuolization in CuO NP-treated rice roots,[50] and Liu *et al.*'s report of concentration-dependent decreases in mitotic activity following CuO NP exposure.[51] Our results thus corroborate the established paradigm that exogenous nanoparticles can disrupt the cellular division process in root meristems.

### 3.3 Effects on oxidative stress of primary roots

Evans blue dye was used as a viability assay for rice primary roots. No significant reduction in the viability of rice primary root cells was observed at AgNPs concentrations below 1.0 mg $L^{-1}$. However, treatments with 5.0 and 10.0 mg $L^{-1}$ AgNPs significantly reduced cell viability by 35% and 63.2%, respectively (Fig. 3A). Malondialdehyde (MDA) serves as a biomarker of lipid peroxidation, reflecting the degree of oxidative damage to cell membranes.[52] As shown in Fig. 3B, the MDA content in rice primary roots increased with rising

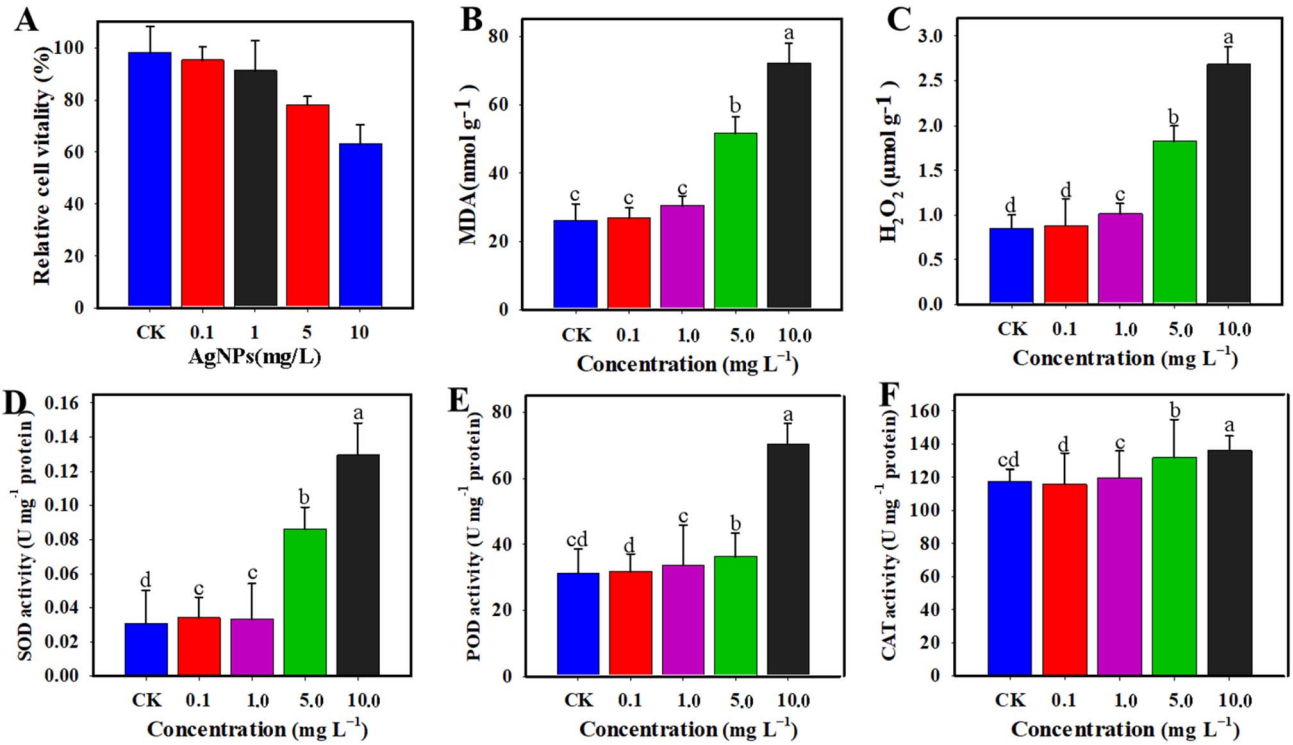


Fig. 3 AgNPs@PEI exposure induces oxidative stress and inhibits root activity in rice primary roots. The effects on (A) root activity, (B) MDA content, (C) $H_2O_2$ content, (D) SOD activity, (E) POD activity, and (F) CAT activity are shown. Error bars indicate standard deviation of the mean ($n = 3$), values are presented as mean ± SD. Samples with a different letter were significantly different ($P < 0.05$), as determined using the Duncan LSD test.

concentrations of AgNPs treatment. Exposure to 10.0 mg $L^{-1}$ AgNPs resulted in a significant elevation of MDA levels from 26.2 ± 5.12 nmol $g^{-1}$ in the control (CK) group to 72.6 ± 5.86 nmol $g^{-1}$, indicating that high concentrations of AgNPs@PEI induce membrane lipid peroxidation damage in rice primary roots. $H_2O_2$ functions not only as an indicator of oxidative stress but also as a crucial signaling molecule that activates the antioxidant defense cascade in plants.[53] As shown in Fig. 3C, AgNPs treatment significantly promoted the accumulation of hydrogen peroxide ($H_2O_2$) in rice primary roots. Exposure to 5 mg $L^{-1}$ AgNPs@PEI resulted in a 2.14-fold increase in $H_2O_2$ content compared with the control (CK) group. The accumulation of $H_2O_2$ can induce oxidative damage and membrane lipid peroxidation in plant tissues, which further explains the elevated MDA levels observed in primary roots upon AgNPs exposure.[54]

Exposure to AgNPs@PEI significantly enhanced antioxidant enzyme activities in rice primary roots, including SOD, POD, and CAT (Fig. 3D–F). Notably, SOD activity displayed a concentration-dependent response, with significant elevation observed at AgNPs@PEI concentrations ≥5.0 mg $L^{-1}$. The highest SOD activity (129.52 ± 18.6 U $g^{-1}$) was recorded at 10 mg $L^{-1}$ treatment. This elevated SOD activity represents a critical defense mechanism against AgNPs@PEI-induced oxidative stress in rice primary roots. Parallel to SOD dynamics, POD activity showed a concentration-dependent increase, rising from 21.23 U $mg^{-1}$ in controls to 36.2 ± 7.36 U $mg^{-1}$ at 5 mg $L^{-1}$ AgNPs@PEI, and further escalating to 70.31 ± 6.43 U $mg^{-1}$ at 10.0 mg $L^{-1}$. While CAT activity in rice primary roots exhibited an increasing trend at both 5.0 and 10.0 mg $L^{-1}$ AgNPs@PEI compared to the control, the changes were statistically non-significant, contrasting with the marked responses of SOD and POD. The coordinated upregulation of POD, CAT, and SOD activities in rice primary roots represents a canonical antioxidant defense mechanism against AgNPs@PEI-induced ROS generation.[55,56] This enzymatic response pattern, well-documented during oxidative stress, directly correlates with elevated lipid peroxidation levels, confirming the activation of primary roots oxidative stress pathways under AgNPs@PEI exposure.

### 3.4 Transcriptomic analysis

**3.4.1 Differential gene expression analysis.** To elucidate the molecular mechanisms underlying the effects of AgNPs@PEI on rice primary root growth, transcriptomic sequencing analysis was conducted to compare the differential gene expression between the control group (CK) and those exposed to 5 mg $L^{-1}$ (abbreviated as AgNPs1) or 10 mg $L^{-1}$ (abbreviated as AgNPs2) AgNPs@PEI treatments. High-throughput sequencing generated high-quality data, with all samples yielding between 34.8 and 43.2 million clean reads and demonstrating excellent sequencing quality (Q20 scores >97.66%), confirming the high quality and reliability of the sequencing data (Table S1).

To identify differentially expressed genes, the expression level of each gene was calculated as FPKM (Fragments Per Kilo bases per Million fragments) based on universal reads. All

uniquely mapped reads were converted to FPKM values using Cufflinks for subsequent comparative analysis (Fig. S4A). Principal component analysis (PCA) revealed clear separation between the control (CK) and AgNPs@PEI treatment groups, demonstrating distinct genome-wide expression profiles (Fig. S4B).

Using Pearson's correlation coefficient analysis, we constructed a correlation heat map to evaluate the association among the three experimental groups (Fig. 4). The results showed that the three groups have good correlation and good biological repeatability. To visualize the differential gene expression responses of rice primary roots to AgNPs exposure, the differentially expressed genes (DEGs) between AgNPs1/CK and AgNPs2/CK comparisons were identified using stringent criteria (adjusted $p$-value < 0.05 and $|\log_2\text{Fold Change}| \geq 1$, corresponding to a minimum 2-fold change). Volcano plots were subsequently generated by plotting gene relative abundance against $p$-value (Fig. S6).

Compared to the CK, AgNPs1 treatment induced significant upregulation of 1262 unigenes and downregulation of 993 unigenes, while AgNPs2 treatment resulted in more pronounced changes with 2877 upregulated and 1535 downregulated unigenes. Furthermore, AgNPs2 treatment showed 1556 upregulated and 348 downregulated unigenes relative to AgNPs1 (Fig. S5A). Venn diagram analysis identified 486 DEGs common to all three comparison groups. The pairwise comparisons revealed group-specific responses: AgNPs1 *vs.* CK contained 423 unique DEGs, AgNPs2 *vs.* CK showed 1727 unique DEGs, and AgNPs2 *vs.* AgNPs1 exhibited 283 unique DEGs (Fig. S5B).

**3.4.2 GO and KEGG pathway analysis of DEGs.** GO offers a set of dynamic, controlled, and structured terminologies to describe gene functions and products in any organism. Under AgNPs@PEI exposure, DEGs are enriched as GO terms. As shown in Fig. 5, the top 20 significant terms are mainly based on three categories: molecular function (MF), cellular component (CC), and biological process (BP). GO enrichment analysis of the DEGs in AgNPs1 *vs.* CK showed that they were more enriched into cell periphery (GO:0071944), extracellular region (GO:0005576), cell wall (GO:0005618), external encapsulating structure (GO:0030312), plasma membrane (GO:0005886), transmembrane transport (GO:0055085), and catalytic activity (GO:0003824) (Fig. 5A). The DEGs in AgNPs2 *vs.* CK were more enriched into extracellular region (GO:0005576), cell wall (GO:0005618), external encapsulating structure (GO:0030312), tetrapyrrole binding (GO:0046906), and heme binding (GO:0020037) (Fig. 5B). The DEGs in AgNPs2 *vs.* AgNPs1 were more enriched into cell periphery (GO:0071944), plasma membrane (GO:005886), extracellular region (GO:0005576), membrane (GO:0016020), intrinsic component of membrane (GO:00031224), and catalytic activity (GO:0003824) (Fig. 5C). Previous transcriptomic investigations have established that AgNPs elicit distinct gene expression profiles in plants. Kaveh *et al.* demonstrated that exposure to 5 mg $L^{-1}$ AgNPs resulted in 286 upregulated and 81 downregulated genes in *Arabidopsis*, with only 13–21% overlap with $Ag^{+}$-responsive genes, suggesting that the majority of transcriptional responses are specific to the nanoparticulate form.[57] Furthermore, Kohan-Baghkheirati and Geisler-Lee uncovered 111 genes that were exclusively responsive to AgNPs and not regulated by other abiotic stressors (cold,

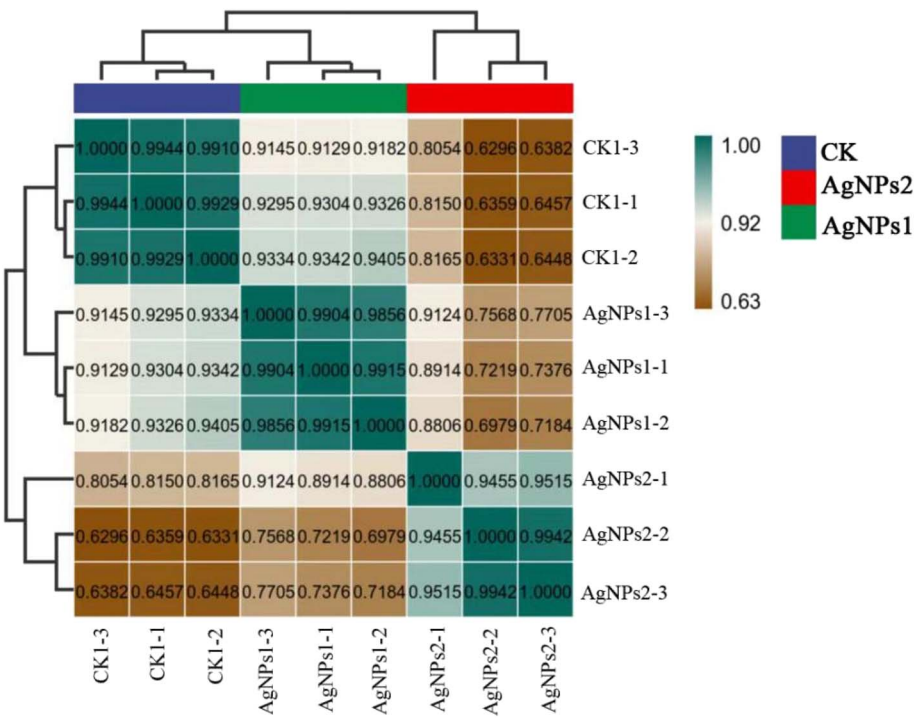


Fig. 4 The Pearson correlation analysis in rice primary root after exposure to AgNPs treatment and CK for 3 days (CK: control AgNPs1: 5 mg $L^{-1}$ AgNPs 2: 10 mg $L^{-1}$).

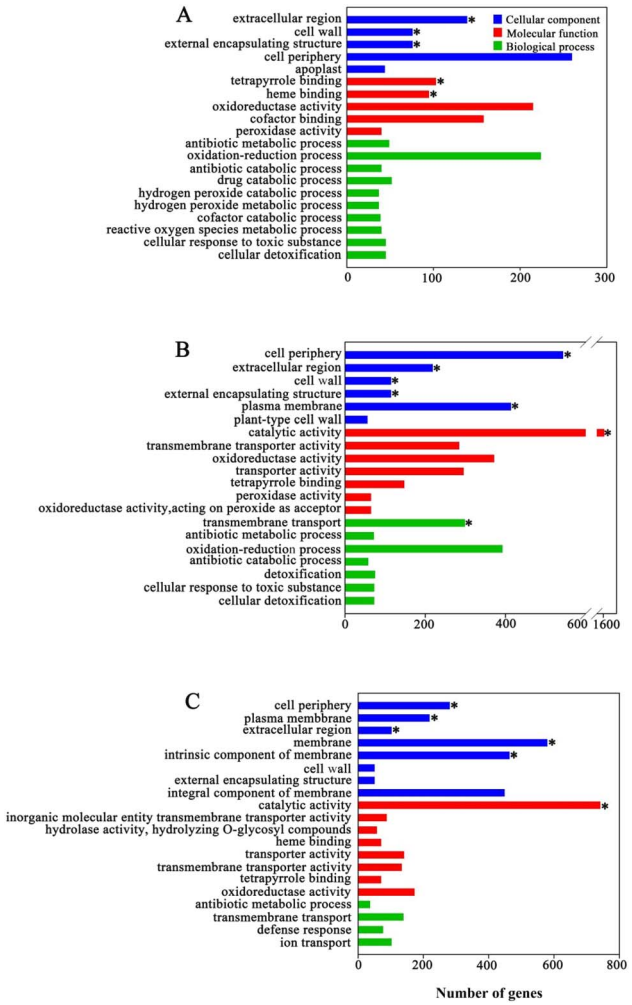


Fig. 5 GO enrichment analysis (A) AgNPs1 *vs.* CK (B) AgNPs2 *vs.* CK (C) AgNPs2 *vs.* AgNPs1 (AgNPs1: 5.0 mg $L^{-1}$ AgNPs2: 10.0 mg $L^{-1}$).

salt, drought, heat).[58] These genes were found to be enriched in three key biological functions: response to fungal infection, anion transport, and cell wall/plasma membrane-related processes. These findings underscore that AgNPs operate through nanoparticle-specific mechanisms beyond simple $Ag^{+}$ ion toxicity.

In order to further study the differential genes, KEGG pathway analysis was performed. The top 20 significantly enriched pathways from three comparison groups were selected for bubble plot visualization. It was found that phenylpropanoid biosynthesis (osa00940), lipid metabolism (osa01040, osa00062), glutathione metabolism (osa00480), and amino acid metabolism (osa00400, osa00460, osa00280, osa00350) were consistently significantly enriched across all three comparisons (Fig. S7).

In the phenylpropanoid biosynthesis pathway (Fig. S8), the comparison groups exhibited significant enrichment of 52 (44 up-regulated, 8 down-regulated), 73 (62 up-regulated, 11 down-regulated), and 32 (28 up-regulated, 4 down-regulated) genes, respectively. These enriched genes encode key enzymes, including 4-coumarate-CoA ligase (4CL), cinnamoyl-CoA reductase (CCR), and cinnamyl alcohol dehydrogenase (CAD). The results indicate that CYP84A plays a central role in catalyzing the conversion of ferulic acid to 5-hydroxyferulate and its downstream derivatives, namely sinapoyl-CoA, sinapaldehyde and sinapyl alcohol. This pathway ultimately leads to the biosynthesis of lignin monomers: guaiacyl lignin, 5-hydroxyguaiacyl lignin, and syringyl lignin.

The transcriptomic profiling revealed that AgNPs@PEI exposure induced extensive reprogramming of glutathione S-transferase (GST) genes in rice primary roots, with 10, 20, and 13 GST-related genes significantly upregulated, and 2, 2, and 1 genes downregulated, across the three comparative groups, respectively (Fig. S9). These findings indicate substantial activation of glutathione metabolism, a critical cellular defense mechanism. GSTs constitute a multifunctional protein family involved in abiotic stress defense, metal detoxification, and auxin homeostasis regulation.[59,60] Previous studies have demonstrated that specific GST isoforms (*e.g.*, *Arabidopsis* AtGSTU17, *sorghum* SbGSTU, and *Lycium barbarum* LbGST1/LbGST) enhance stress tolerance through modulation of antioxidant enzyme activity and maintenance of cellular redox homeostasis.[61–63] Therefore, we hypothesize that the observed upregulation of GST-related genes contributes to the enhanced tolerance of rice primary roots to AgNPs@PEI exposure *via* improved detoxification capacity and redox balance.

### 3.5 The primary root cell metabolomics in response to AgNPs

**3.5.1 Identified metabolites and differential metabolites analysis.** Through non-targeted LC-MS/MS metabolomics, the global metabolic responses of rice primary roots to AgNPs@PEI exposure were investigated. Multivariate analysis (PCA and PLS-DA) revealed clear metabolic distinctions between control and treated groups (Fig. S10), confirming AgNPs@PEI-induced metabolic reprogramming. PLS-DA modeling (VIP>1, $p < 0.05$) identified 493 DEMs (Fig. S11) with distinct response patterns: AgNPs1 treatment altered 208 metabolites (112 metabolites up-regulated/96 metabolites down-regulated) relative to control, while AgNPs2 affected 172 metabolites (97 metabolite up-regulated/76 metabolites down-regulated). Comparative analysis between AgNPs2 and AgNPs1 groups revealed 113 differentially regulated metabolites (64 metabolites up-regulated/49 metabolites down-regulated). Hierarchical clustering (Fig. S12) classified these DEMs into four major categories: lipids (26.41%), amino acids (14.11%), carbohydrates (8.27%) and nucleotides (4.84%), demonstrating the systemic metabolic disruption caused by AgNPs@PEI in rice primary roots.

**3.5.2 Pathway analysis of DEMs.** To delineate the metabolic responses to AgNPs exposure in primary roots, KEGG functional annotation and pathway enrichment analyses were conducted. As illustrated in Fig. S13, eight, thirteen, and two significantly enriched metabolic pathways ($P < 0.05$) across different treatment groups were identified under different treatment conditions, with five core pathways consistently perturbed: (1) unsaturated fatty acid biosynthesis, (2) ABC transporters, (3) pyrimidine metabolism, (4) TCA cycle, and (5) alanine/

aspartate/glutamate metabolism. The identified pathways were closely linked to 24 differentially expressed metabolites (DEMs), comprising: (i) six amino acids involved in nitrogen metabolism, (ii) four carbohydrates central to energy homeostasis, (iii) six fatty acids critical for membrane integrity, and (iv) eight nucleotides essential for nucleic acid metabolism.[64] The 24 identified DEMs, whose relative abundance profiles are presented in Fig. 6, include six amino acids, particularly noteworthy given their established role as sensitive metabolic indicators of stress responses in plants. Numerous studies have demonstrated that amino acids frequently undergo significant concentration changes when plants encounter environmental stressors[65–67] In this study, we observed significant alterations in the relative abundance of GABA, DL-glutamic acid, alanine, argininosuccinic acid, L-leucine, and L-proline in both AgNPs1 and AgNPs2 treatment groups. Notably, DL-glutamic acid exhibited an upward trend in the osa00330 metabolic pathway when comparing AgNPs2 *vs.* CK and AgNPs2 *vs.* AgNPs1. As a pivotal amino acid in protein metabolism, glutamic acid exerts dual effects on the growth and development of rice primary roots. On one hand, insufficient glutamic acid supply reduces protein synthesis efficiency, thereby failing to meet the protein demands for rice primary root growth and consequently exerting detrimental effects.[68] On the other hand, as an acidic amino acid, glutamic acid accumulation alters the extracellular pH environment, creating an acidic environment that inhibits root growth. Previous studies have demonstrated that elevated glutamic acid concentrations inhibit primary root growth in both *Arabidopsis* and rice.[69–72] We therefore hypothesize that overexpression of glutamic acid may suppress rice primary root growth. The unsaturated fatty acids, including α-linolenic acid, docosahexaenoic acid, and oleic acid, exhibited decreased levels in the three comparison groups. The saturated fatty acids, behenic acid and stearic acid, showed similar downward trends, with only palmitic acid expression increasing. Increased fatty acid unsaturation enhances cell membrane fluidity.[73,74] As the three groups of comparative results show that the levels of both saturated and unsaturated fatty acids are down-regulated, it can be concluded that AgNPs negatively impacted the cell membrane fluidity of rice primary roots, thus disrupting critical cellular activities such as material transport, energy conversion, and signal transduction across the membrane.[75,76]

### 3.6 Analysis of the key metabolic pathway

Through integrated transcriptomic and metabolomic profiling, we systematically investigated several critical metabolic pathways implicated in cellular structural integrity: (i) carbohydrate metabolism pathways (galactose metabolism, KEGG osa00052), (ii) protective lipid biosynthesis pathways (cutin/suberin/wax biosynthesis, osa00073 and glycerophospholipid metabolism, osa00564), and (iii) stress-responsive nitrogen metabolism pathways (arginine/proline metabolism, osa00330 and purine metabolism, osa00230). While metabolomic investigations of AgNPs effects on rice roots remain limited, studies in wheat, a closely related monocot, have demonstrated that AgNPs exposure reduces galactose levels in roots, impairing the synthesis of arabinogalactans critical for cell wall integrity.[77] This is consistent with our observation of galactose metabolic network disruption and mannose fluctuation in rice primary roots, suggesting conserved mechanisms of nanoparticle-induced cell wall damage in cereals.

Fig. 7 illustrates profound disturbances in galactose metabolism in rice primary roots under AgNPs@PEI exposure, characterized by: (i) substantial transcriptional reprogramming (10, 15, and 6 DEGs across the three comparison groups), (ii) metabolic flux alterations (3, 2, and 4 DEMs), and (iii) consistent accumulation of inositol galactosides. Specifically, the persistent upregulation of galA ($\log_2$FC > 2.0, $p < 0.01$ in all groups) highlights its central regulatory function in maintaining galactose homeostasis during nanoparticle stress. Mechanistically, the elevated inositol galactoside levels, a hallmark of raffinose family oligosaccharide metabolism, likely serve dual physiological roles: as osmoprotectants maintaining cellular turgor pressure through osmotic adjustment, and as signaling molecules modulating membrane permeability to preserve cellular integrity under stress conditions. These coordinated responses between galA-mediated transcriptional control and GOLS-associated metabolic adjustments demonstrate a sophisticated adaptation mechanism in the galactose metabolic network. Moreover, the integrated analysis reveals that AgNPs exposure significantly perturbs key metabolic components involved in cell wall-associated carbohydrate homeostasis.[78,79] Specifically, mannose, a structural hexose critical for hemicellulose formation and cell wall assembly through its interactions with cellulose and pectin,[80] exhibited contrasting regulation patterns, significant downregulation under AgNPs1 treatment *versus* marked upregulation with AgNPs2 exposure. This response was accompanied by dynamic fluctuations in galactinol and sucrose levels, suggesting their involvement in both cell wall remodeling and osmotic adjustment. Concurrently, activation of the α-galactosidase-encoding gene malZ drove galactose catabolism, leading to significant accumulation of melibiose, while upregulation of sucrose invertase promoted sucrose hydrolysis into D-fructose. These multi-faceted effects ultimately disrupt the galactose metabolic network, compromise energy supply, and destabilize cell wall integrity during early root growth, revealing the sophisticated metabolic toxicity of AgNPs exposure in primary root.

Our integrated omics analysis revealed that AgNPs@PEI exposure significantly reprogrammed protective lipid biosynthesis in rice primary roots, with distinct molecular signatures observed for cutin, suberin, and wax pathways (Fig. 8). Specifically, transcriptomic profiling identified 9, 11, and 4 DEGs significantly enriched in these pathways, respectively, while metabolomic analysis detected 5, 5, and 0 corresponding DEMs, demonstrating a predominant transcriptional regulation over metabolic alteration. These protective lipids serve distinct yet complementary structural functions: cutin and wax form hydrophobic surface barriers that minimize water loss and provide defense against pathogen invasion,[81] whereas suberin, a complex polymer containing fatty acids and phenolic components (notably sinapic acid and coumarins), is strategically deposited between the plasma membrane and cell wall to

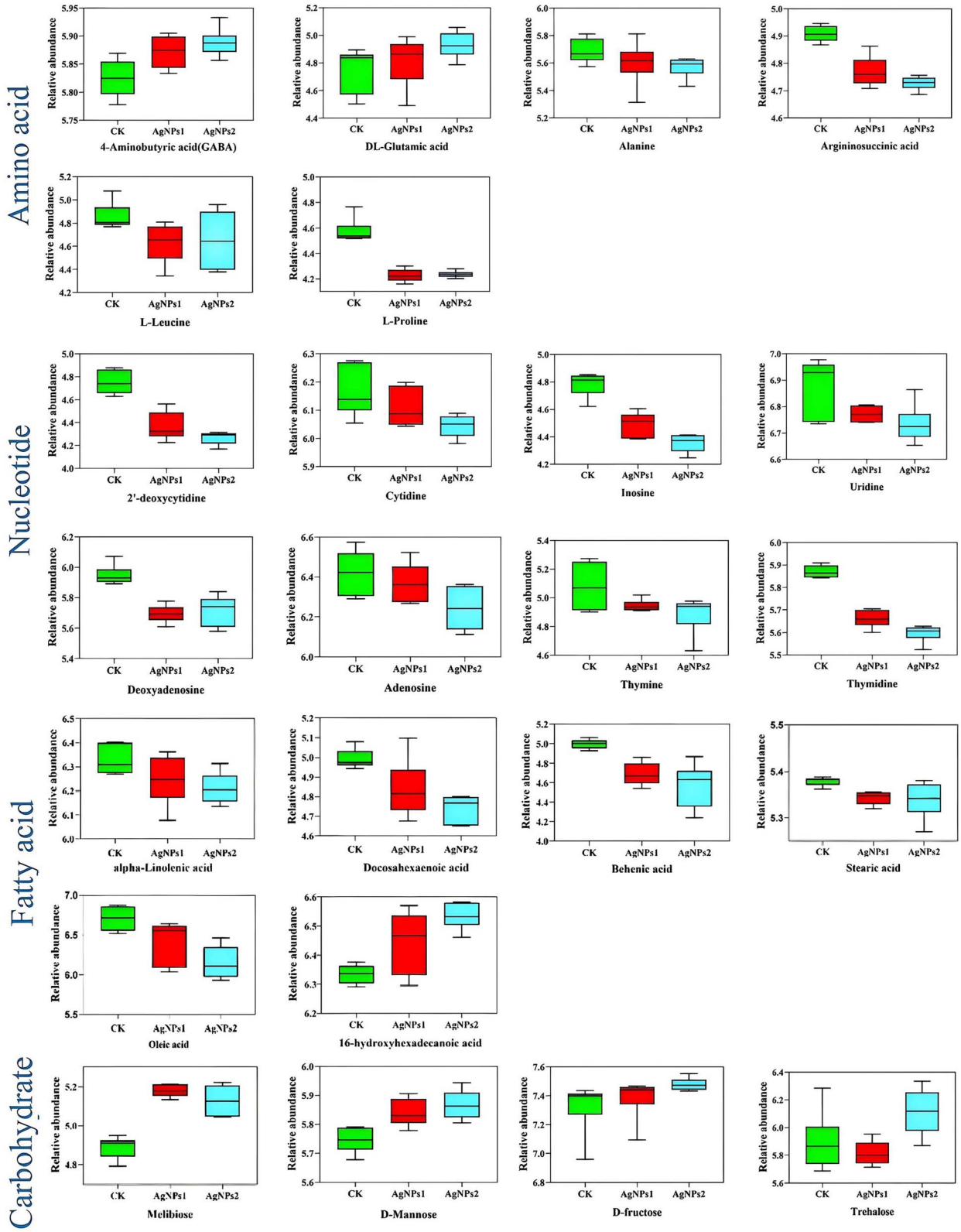


Fig. 6 The box plots display the relative abundance of amino acids, nucleotides, fatty acids, and carbohydrates across the 24 differentially expressed metabolites (DEMs) identified. The center line inside the box represents the median, while the lower and upper bounds of the box indicate the 25th and 75th percentiles, respectively. The whiskers represent the entire data range (minimum and maximum). All data are based on $n = 6$ biological replicates per group (AgNPs1: 5.0 mg $L^{-1}$ AgNPs2: 10.0 mg $L^{-1}$).

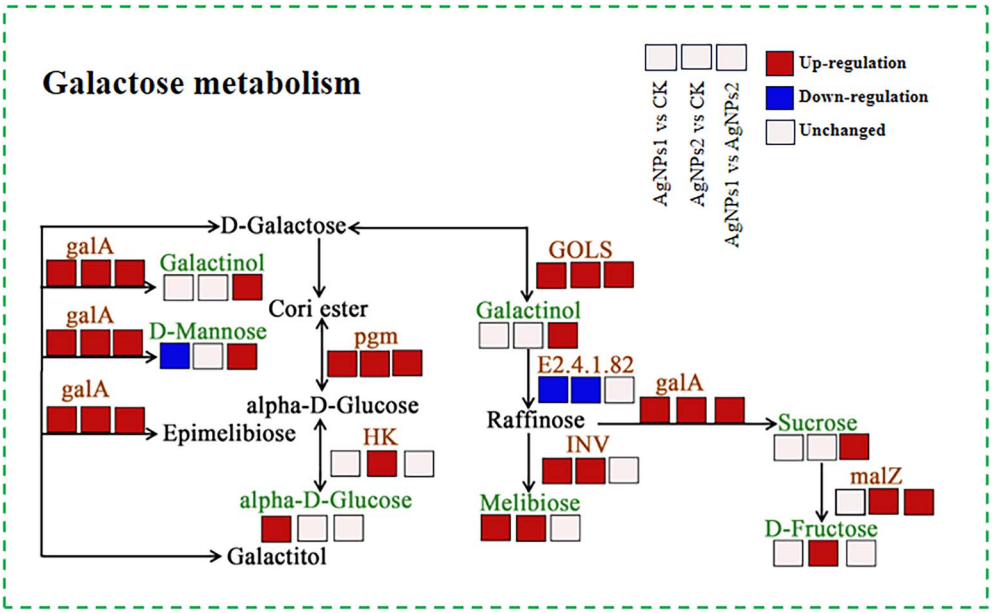


Fig. 7 Schematic diagram of rice primary root galactose metabolism.

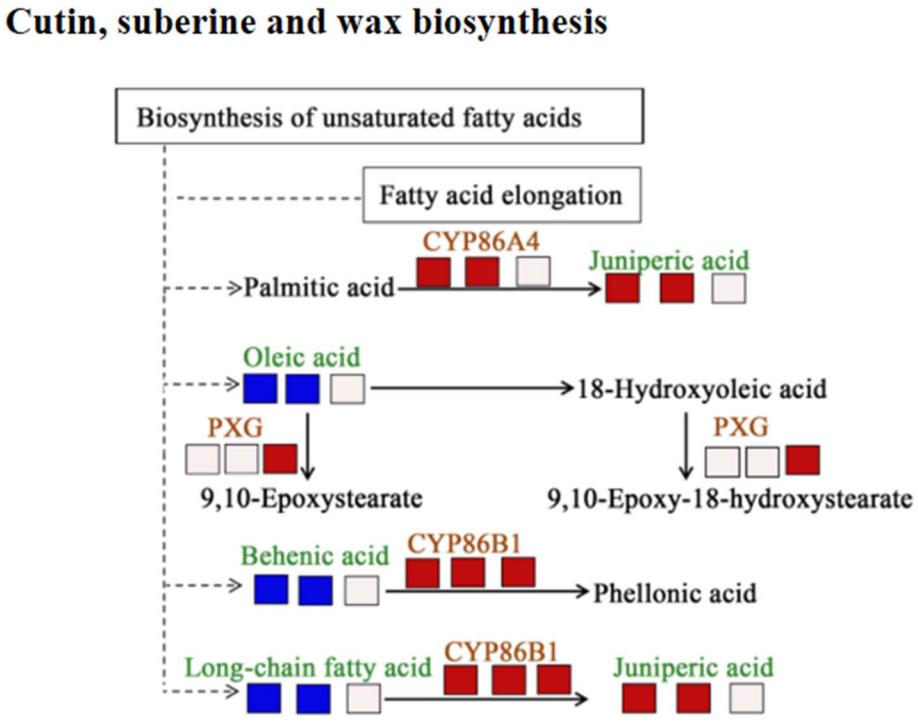


Fig. 8 Schematic diagram of rice primary root cutin, suberin and wax biosynthesis.

reinforce cellular boundaries under stress.[82,83] The observed differential regulation of these pathways suggests that AgNPs@PEI triggers active cell wall remodeling responses in primary roots. Previous studies have demonstrated that cytochrome P450 enzymes, particularly CYP86A1 and CYP86B1, are specifically highly expressed in the endodermal tissues of *Arabidopsis thaliana*.[84–86] These enzymes play pivotal roles in the suberin biosynthesis pathway. Specifically, CYP86A1 contributes to suberin formation by catalyzing the generation of ω-hydroxy fatty acid monomers, a function that has been experimentally confirmed in both *Arabidopsis* roots and potato tuber periderm.[87] As shown in Fig. 8, we identified significant upregulation of CYP86A4 and CYP86B1 homologs in rice following AgNPs@PEI exposure. It has been proposed that under abiotic stress conditions, CYP86A1 and CYP86B1 are transcriptionally activated by heavy metals and drought, functioning as

molecular switches that convert the endodermis from a passive barrier into an active, stress-reinforced shield.[88,89] In the present study, the marked induction of CYP86A4 and CYP86B1 homologs in AgNPs@PEI-exposed rice roots indicates that silver nanoparticles trigger this conserved barrier-reinforcement program. The resulting suberin accumulation likely constitutes a pathological sealing of the endodermis, disrupting the apoplastic transport of water and nutrients and contributing to the observed growth inhibition in primary roots.

The structural integrity of biological membranes relies on glycerophospholipid bilayers, which are constructed through the glycerol-3-phosphate backbone. Metabolomic analysis revealed that sodium glycerol-3-phosphate levels were significantly downregulated in both AgNPs1 and AgNPs2-treated groups compared to CK (Fig. 9). This reduction in a key metabolic intermediate disrupts glycerophospholipid biosynthesis, ultimately compromising cellular membrane stability.[90] Phospholipase C (*Os03g0852800*, *OsNPC3*) and lysophosphatidylcholine (LPC) were significantly upregulated across three comparative groups, suggesting that AgNPs@PEI substantially disrupts membrane lipid remodeling and signal transduction processes. While LPC plays a crucial role in regulating membrane fluidity and cellular signaling, excessive accumulation can induce membrane destabilization and even trigger cell death.[91,92] In contrast, phosphatidylcholine (PC) showed significant upregulation only in the AgNPs1 *vs.* CK comparison, with no differential regulation observed in AgNPs2 *vs.* CK. This lack of response at higher exposure levels (AgNPs2) may indicate that the stress threshold for PC-mediated membrane adaptation was exceeded in the rice seminal root. These observations suggest either membrane lipid peroxidation damage or the activation of specific stress-responsive signaling pathways.

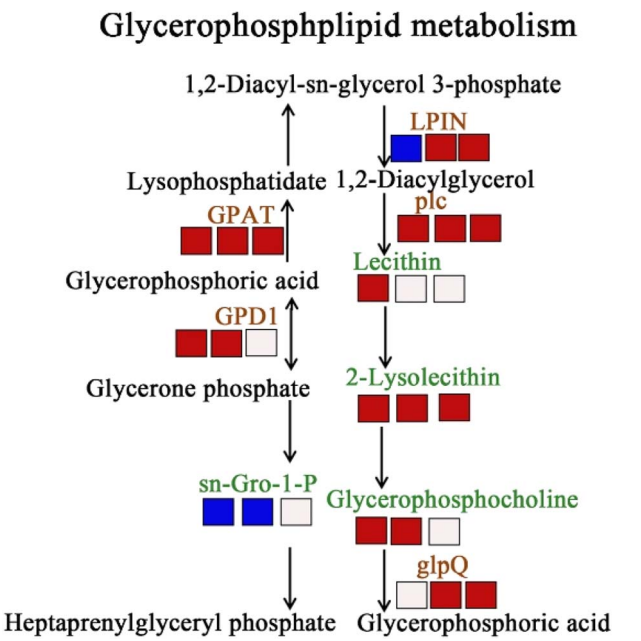


Fig. 9 Schematic diagram of rice primary root glycerophospholipid metabolism.

Amino acids serve as crucial energy-related metabolites in plants, participating in diverse physiological processes including hormone regulation, energy metabolism, and cellular growth.[93] Substantial evidence demonstrates their pivotal roles in plant stress responses to various abiotic challenges, including metal toxicity and drought conditions.[94,95] Our analysis revealed significant alterations in arginine metabolism across all three comparative groups, with 3, 9, and 7 DEGs and 4, 5, and 2 DEMs identified, respectively. Similarly, proline metabolism showed notable changes, with 9, 7, and 5 DEGs and 5, 2, and 4 DEMs detected (Fig. 10). Interestingly, while the peptide metabolite pip was consistently upregulated across all groups, both metabolic abundance and transcriptional levels of proline displayed decreasing trends. This finding is particularly noteworthy given proline's well-established function in maintaining cellular osmotic balance, stabilizing membrane-associated protein structures, and preventing membrane deformation.[96,97] Therefore, the reduction in proline content may affect the morphological structure of the cell membrane in

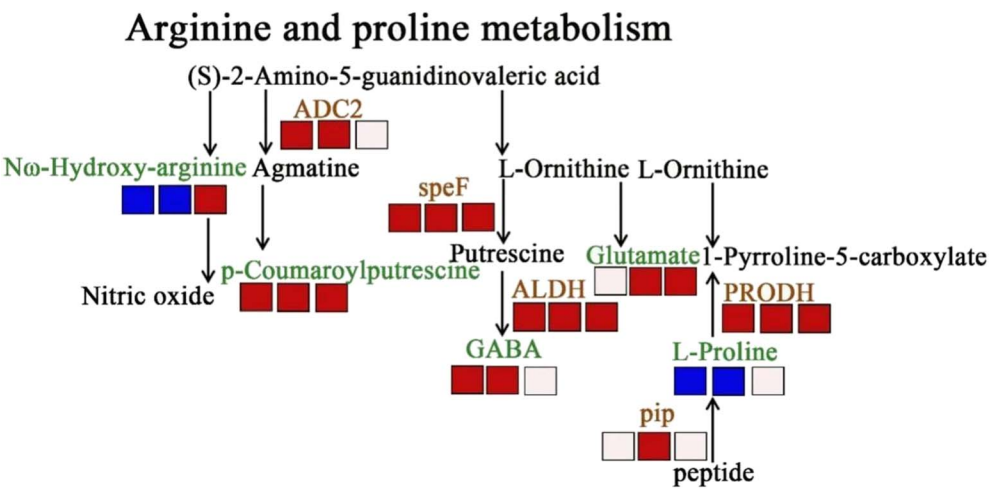


Fig. 10 Schematic diagram of rice primary root arginine and proline metabolism.

rice primary roots. Furthermore, aldehyde dehydrogenase (ALDH) was significantly expressed in all three groups, and γ-aminobutyric acid (GABA) was significantly upregulated in the AgNPs treatment group. GABA accumulation represents a well-documented physiological response to diverse abiotic stresses, including water deficit, temperature extremes, and salinity.[98,99] In *Arabidopsis*, elevated GABA levels have been shown to downregulate genes involved in secreted protein production and cell wall biosynthesis, ultimately resulting in root cell elongation defects. The phenotypic effects of GABA likely result from its complex interplay with phytohormones such as ABA and ethylene.[100] Based on these observations, we propose that growth inhibition induced by AgNPs in rice primary roots may be mediated, at least in part, by GABA overexpression disrupting hormonal homeostasis. This perturbation could potentially alter the balance between root growth promotion and inhibition pathways.

Purine metabolism represents a key metabolic pathway for plant growth and development, participating in both precursor synthesis for DNA/RNA and diverse physiological and metabolic processes in cells.[101,102] In the purine metabolism pathway, there are 8, 9, 1 DEGs and 5, 5, 2 DEMs were significantly enriched, respectively (Fig. 11). Among DEMs identified, the relative abundance of nucleotide-related compounds all exhibited decline including cytidine, inosine, uridine, deoxycytidine, adenosine, thymidine, and thymine (Fig. 6). The upregulation of adenosine deaminase (ADA) across all groups led to down-regulation of its substrate, hypoxanthine nucleoside, in AgNPs-treated groups. Concurrently, increased transcriptional levels of phosphoglucomutase (pgm) and accumulation of its product ribose-5-phosphate indicated activation of the purine salvage synthesis pathway to sustain energy supply. Collectively, AgNPs disrupt energy homeostasis in purine metabolism, driving adaptive metabolic reprogramming to mitigate toxicity.

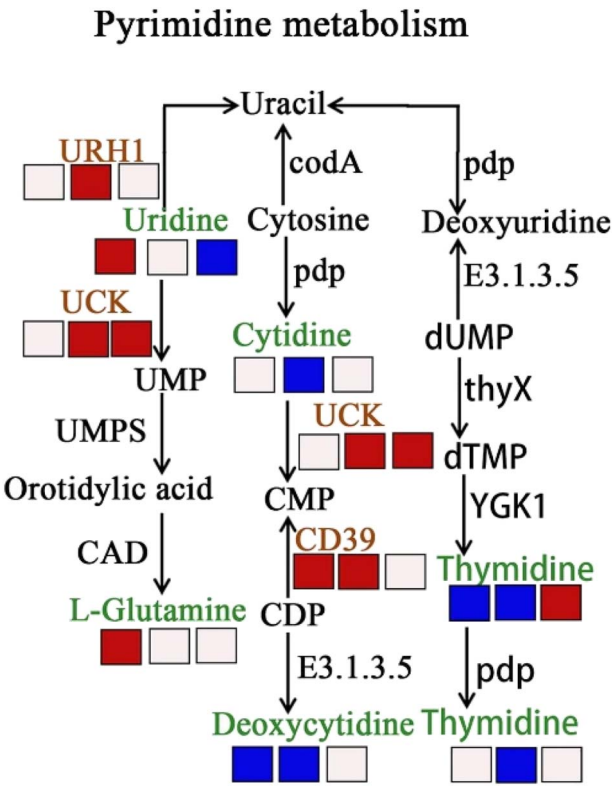


Fig. 11 Schematic diagram of rice primary root purine metabolism.

# 4 Conclusion

This study systematically elucidated the phytotoxic mechanisms of AgNPs in rice primary roots through integrated morphological, physiological, and molecular levels. Exposure to AgNPs disrupted the physiological metabolism of rice primary roots, leading to growth inhibition. Transcriptomic profiling revealed that DEGs were predominantly enriched in pathways related to transmembrane transport, redox enzyme activity in the cell wall, and external encapsulating structure formation. Metabolomic analysis demonstrated that AgNPs exposure significantly altered metabolic pathways, particularly those involving amino acids, organic acids, nucleic acids, and carbohydrates. Notably, AgNPs compromised energy supply for early root growth by disrupting galactose metabolism. Comprehensive analysis revealed that AgNPs-induced impairment of cell wall and membrane growth primarily stems from disruptions in critical metabolic pathways, including phenylpropanoid biosynthesis, amino acid metabolism, galactose and carbohydrate metabolism, and glycerophospholipid metabolism. These findings provide novel insights into the phytotoxicity of AgNPs from the perspective of plant primary tissues. Given the absence of control groups for dissolved silver ions and the PEI coating, the effects observed on primary roots in this study should be interpreted as the integrated biological response to AgNPs@PEI. Further research is needed to quantitatively distinguish the contributions of the nanoparticles themselves, dissolved silver ions, and the PEI coating. In addition, we will further investigate the effects of AgNPs with varying surface modifications on rice primary roots and validate the impact of AgNPs on primary root development under soil conditions, thereby providing a more comprehensive and generalized understanding of the underlying mechanisms.

## Author contributions

Jiajia Yang: methodology, experimental design. Ruihua Chen: experimental operation, analysis, writing – original draft. Huan Zhang: formal analysis. Ruonan Wang: data curation. Zhifeng Zhang: manuscript revision.

## Conflicts of interest

The authors declare that they have no known competing financial interests or personal relationships that could have appeared to influence the work reported in this paper.

## Data availability

The raw RNA-seq data generated in this study are available in the NCBI SRA under accession number PRJNA1359025. The

untargeted metabolomics raw data have been deposited in the MetaboLights repository under accession number MTBLS13693.

Supplementary information (SI): the data and information, have been clearly indicated in the corresponding sections of the main text. See DOI: https://doi.org/10.1039/d5ra05319f.

## Acknowledgements

This work was supported by the Natural Science Foundation of Shanxi Province (202203021221123), the Scientific Research Foundation for the Returned Overseas Chinese Scholar, Shanxi Province (2022-122) and Innovative Project of Graduate Education in Shanxi Normal University (2024XSY54).

## References

1 K. A. Johnston, N. A. Diemler, V. S. Cooper, J. E. Millstone, S. J. Haig and L. M. Gilbertson, Role of bacterial motility in differential resistance mechanisms of silver nanoparticles and silver ions, *Nat. Nanotechnol.*, 2021, **16**, 996–1003.

2 S. Budhani, N. P. Egboluche, Z. Arslan, H. Yu and H. Deng, Phytotoxic effect of silver nanoparticles on seed germination and growth of terrestrial plants, *J. Environ. Sci. Health.*, 2019, **37**, 330–355.

3 L. Wang, J. Sun, L. Lin, Y. Fu, H. Alenius, K. Lindsey and C. Chen, Silver nanoparticles regulate *Arabidopsis* root growth by concentration-dependent modification of reactive oxygen species accumulation and cell division, *Ecotox. Environ. Safe.*, 2019, **190**, 110072.

4 T. A. Yekeen, M. A. Azeez, A. Akinboro, A. Lateef, T. B. Asafa, I. C. Oladipo, S. O. Oladokun and A. A. Ajibola, Safety evaluation of green synthesized *Cola nitida* pod, seed and seed shell extract-mediated silver nanoparticles (AgNPs) using an *Allium cepa* assay, *J. Taibah. Univ. Sci.*, 2018, **11**, 895–909.

5 L. Yin, B. P. Colman, B. M. Mcgill, J. P. Wright and E. S. Bernhardt, Effects of Silver Nanoparticle Exposure on Germination and Early Growth of Eleven Wetland Plants, *PlosOne*, 2012, **7**, e47674.

6 F. Mirzajani, H. Askari, S. Hamzelou, M. Farzaneh and A. Ghassempour, Effect of silver nanoparticles on *Oryza sativa* L and its rhizosphere bacteria, *Ecotox. Environ. Safe.*, 2013, **88**, 48–54.

7 H. Lequeux, C. Hermans, S. Lutts and N. Verbruggen, Response tocopper excess in *Arabidopsis thaliana*: Impact on the root system architecture, hormone distribution, ligninaccumulation and mineral profile, *Plant. Physiol. Biochem.*, 2010, **48**, 673–682.

8 M. Ke, Q. Qu, W. J. G. M. Peijnenburg, X. Li, M. Zhang, Z. Zhang, T. Lu, X. L. Pan and H. Qian, Phytotoxic effects of silver nanoparticles and silver ions to Arabidopsis thaliana as revealed by analysis of molecular responses and of metabolic pathways, *Sci. Total. Environ.*, 2018, **644**, 1070–1079.

9 P. M. G. Nair and I. M. Chung, Physiological and molecular level studies on the toxicity of silver nanoparticles in germinating seedlings of mung bean (*Vigna radiata* L.), *Acta. Physiol. Plant.*, 2015, **37**, 1719.

10 M. Rui, C. Ma, X. Tang, J. Yang, F. Jiang, Y. Pan, Z. Xiang, Y. Hao, Y. Rui, W. Cao and B. Xing, Phytotoxicity of Silver Nanoparticles to Peanut (*Arachis hypogaea* L.): physiological responses and food safety, *ACS. Sustainable. Chem. Eng.*, 2017, **5**, 6557–6567.

11 K. S. Siddiqi and A. Husen, Plant response to silver nanoparticles: a critical review, *Crit. Rev. Biotechnol.*, 2022, **42**, 973–990.

12 A. Q. Chen, Z. Q. Long, Y. Xiao, Y. M. Feng, Y. Zhou, S. Yang, Y. M. Liao, X. Zhou, L. W. Liu, Z. B. Wu and S. Yang, Application of natural product-based quorum sensinginhibitors in plant pathogen control: A review, *Arab. J. Chem.*, 2024, **18**, 106050.

13 O. M. Abdallah, Y. Sedky and H. R. Shebl, Comprehensive evaluation of the antibacterialand antibiofilm activities of NiTi orthodontic wires coated with silver nanoparticles and nanocomposites: an *in vitro* study, *BMC. Oral. Health*, 2024, **24**, 1345.

14 A. Balciunaitiene, V. Januskevice, S. Saunoriute, U. Raubyte, J. Viskelis, P. B. Memvanga and P. Viskelis, Antimicrobial Antioxidant Polymer Films with Green Silver Nanoparticles from *Symphyti radix*, *Polymers*, 2024, **16**, 317.

15 Y. Feng, Q. Sun, P. Liu, W. Fan and B. Fan, Antibacterial Property and Mechanisms of Au@Ag Core-Shell Nanoparticles with Near-Infrared Absorption Against E. *faecalis* Infection of Dentin, *Int. J. Nanomed.*, 2024, **19**, 6981–6997.

16 V. Inácio, R. Santos, R. Prazeres, J. Graça, C. M. Miguel and L. Morais-Cecílio, Epigenetics at the crossroads of secondary growth regulation, *Front. Plant. Sci.*, 2022, **13**, 970342.

17 X. P. Zhang, C. X. Ma, L. R. Sun and F. S. Hao, Roles and mechanisms of $Ca^{2+}$ in regulating primary root growth of plants, *Plant. Signaling. Behav.*, 2020, **15**, 1748283.

18 S. H. Fan, Z. H. Huang, H. F. Liu, X. F. Zhang, W. Hua and Z. W. Fu, Sucrose mediates moderate salinity-promoted primary root growth in rapeseed, *Plant. Physiol. Biochem.*, 2025, **227**, 110133.

19 W. W. Lin, X. Zhou, W. X. Tang, K. Takahashi, X. Pan, J. W. Dai, H. Ren, X. Y. Zhu, S. Q. Pan, H. Y. Zheng, W. M. Gray, T. D. Xu, T. Kinoshita and Z. B. Yang, Tmk-based cell-surface auxin signalling activates cell-wall acidification, *Nature*, 2021, **599**, 278–282.

20 M. Yamada, X. Han and P. N. Benfey, RGF1 controls root meristem size through ROS signalling, *Nature*, 2020, **577**, 85–88.

21 D. Alberto, F. Ramel, C. Sulmon, G. Gouesbet and I. Couée, Differential effects of root-level exposure to triazine xenobiotics on root development plasticity in *Arabidopsis thaliana*, *Acta. Physiol. Plant.*, 2022, **44**, 111.

22 L. Sun, P. Zhang, F. Liu, Q. Ju and J. Xu, Molecular and genetic analyses revealed the phytotoxicity of perfluorobutane sulfonate, *Environ. Int.*, 2022, **170**, 107646.

23 M. Berners-Lee, C. Kennelly, R. Watson and C. N. Hewitt, Current global food production is sufficient to meet

human nutritional needs in 2050 provided there is radical societal adaptation, *Elem. Sci. Anth.*, 2018, **6**, 52.

24 S. Huang, P. T. Wang, N. Yamaji and J. F. Ma, Plant Nutrition for Human Nutrition: Hints from Rice Research and Future Perspectives, *Mol. Plant.*, 2020, **13**, 825–835.

25 J. J. Yang, H. Y. Duan, X. Y. Wang, H. Zhang and Z. F. Zhang, Effects of rice root exudates on aggregation, dissolution and bioaccumulation of differently-charged Ag nanoparticles, *RSC Adv*, 2022, **12**, 9435–9444.

26 W. M. Lee, J. I. Kwak and Y. J. An, Effect of silver nanoparticles in crop plants *phaseolus radiatus* and *sorghum bicolor*: media effect on phytotoxicity, *Chemosphere*, 2012, **86**, 491–499.

27 Q. Q. Yang, W. Xu, G. L. Liu, M. Y. Song, Z. Q. Tan, Y. X. Mao, Y. G. Yin, Y. Cai, J. F. Liu and G. B. Jiang, Transformation and uptake of silver nanoparticles and silver ions in rice plant (*Oryza sativa* L.): the effect of iron plaque and dissolved iron, *Environ. Sci. Nano*, 2020, **7**, 599–609.

28 W. Y. Zhang, Q. Wang, M. Li, F. Dang and D. M. Zhou, Nonselective uptake of silver and gold nanoparticles by wheat, *Nanotoxicology*, 2019, **13**, 1073–1086.

29 J. Kalman, K. B. Paul, F. R. Khan, V. Stone and T. F. Fernandes, Characterisation of bioaccumulation dynamics of three differently coated silver nanoparticles and aqueous silver in a simple freshwater food chain, *Environ. Chem.*, 2015, **12**, 662–672.

30 R. G. Chen, N. Xu, B. Yu, Q. Wu, X. X. Li, G. Wang and J. L. Huang, The WUSCHEL-related homeobox transcription factor OsWOX4 controls the primary root elongation by activating OsAUX1 in rice, *Plant Sci.*, 2020, **298**, 110575.

31 C. Jacyn Baker and N. M. Mock, An improved method for monitoring cell death in cell suspension and leaf disc assays using evans blue, *Plant. Cell. Tissue. Organ. Cult.*, 1994, **39**, 7–12.

32 I. Idrees, A. Razzaq, M. Zafar, A. Umer, F. Mustafa, F. Rehman and W. Y. Kim, Silver (Ag) doped graphitic carbon nitride ($g\text{-}C_3N_4$) photocatalyst for enhanced degradation of Ciprofloxacin (CIP) under visible light irradiation, *Arab. J. Chem.*, 2024, **17**, 105615.

33 C. Jacyn Baker and N. M. Mock, An improved method for monitoring cell death in cell suspension and leaf disc assays using evans blue, *Plant. Cell. Tissue. Organ. Cult.*, 1994, **39**, 7–12.

34 X. Yang, Y. Chen, W. Liu, T. Huang, Y. Yang, Y. Mao and Y. Meng, Combined transcriptomics and metabolomics to analyse the response of *Cuminum cyminum* L. under Pb stress, *Sci. Total. Environ.*, 2024, **923**, 171497.

35 Z. F. Zhang, H. J. Chen, W. M. Wu, W. T. Pang and G. Q. Yan, Efficient removal of Alizarin Red s from aqueous solution by polyethyleneimine functionalized magnetic carbon nanotubes, *Bioresour. Technol.*, 2019, **293**, 122100.

36 C. P. Andersen, G. King, M. Plocher, M. Storm, L. R. Pokhrel, M. G. Johnson and P. T. Rygiewicz, Germination and early plant development of ten plant species exposed to titanium dioxide and cerium oxide nanoparticles, *Environ. Toxicol. Chem.*, 2016, **35**, 2223–2229.

37 E. Skiba, M. Pietrzak, M. Gapińska and W. M. Wolf, Metal Homeostasis and Gas Exchange Dynamics in *Pisum sativum* L. Exposed to Cerium Oxide Nanoparticles, *Int. J. Mol. Sci.*, 2020, **21**, 8497.

38 G. Li, Q. Gao, A. Nyande, Z. Dong, E. H. Khan, Y. Han and H. Wu, Cerium oxide nanoparticles promoted lateral root formation in Arabidopsis by modulating reactive oxygen species and $Ca^{2+}$ level, *Funct. Plant. Biol.*, 2024, **51**, 24196.

39 A. Kumar, A. M. Hussein, F. M. A. Altalbawy, M. Kaur, H. Kaur, S. S. Jalal, S. Hassan Zain Al-Abdeen, K. Muzammil and M. Alhadrawi, Synthesis of $g\text{-}C_3N_4$ decorated with ZIF-8 and $CuFe_2O_4$ as a highly efficient and magnetically separable photocatalystfor degradation of tetracycline, *Arab. J. Chem.*, 2024, **17**, 105912.

40 M. Kumar, K. Seth, S. Choudhary, G. Kumawat, S. Nigam, G. Joshi, V. Saharan, M. Meena and A. K. G. Harish, Toxicity evaluation of iron oxide nanoparticles to freshwater cyanobacteria nostoc *ellipsosporum*, *Environ. Sci. Pollut. Res.*, 2023, **30**, 55742–55755.

41 H. Zafar, A. Ali and M. Zia, CuO Nanoparticles Inhibited Root Growth from *Brassica nigra* Seedlings but Induced Root from Stem and Leaf Explants, *Appl. Biochem. Biotech.*, 2017, **181**, 365–378.

42 W. M. Lee, Y. J. An, H. Yoon and H. S. Kweon, Toxicity and bioavailability of copper nanoparticles to the terrestrial plants mung bean (Phaseolus radiatus) and wheat (Triticumaestivum): plant agar test for water-insoluble nanoparticles, *Environ. Toxicol. Chem.*, 2008, **27**, 1915–1921.

43 W. Liu, B. Su, H. Song, X. Zhang, G. Ren, X. Wang, L. Yan, S. Ma, L. Li, L. Guo, S. Xu, B. Zhang, H. Diao, Z. Wu, S. Li and C. Zhang, Photothermal-triggered release of alkyl radicals hydrogel *via* versatile carbon dots chelating $Ag^{+}$ and its synergistic anti-bacterial and biofilm activities, *Arab. J. Chem.*, 2024, **17**, 105755.

44 L. Mercado-Díaz de León, C. Garcidueñas-Piña, E. Pérez-Molphe-Balch, A. Loera-Muro and J. F. Morales-Domínguez, Effect of BvAgNP on growth, development, and glyoxalase gene expression analysis in *Mammillaria bombycina* and *Selenicereus undatus*,, *Mol. Biol. Rep.*, 2024, **51**, 681.

45 G. Liu, M. Pan, J. Song, M. Guo, L. Xu and Y. Xin, Investigating the effects of biocharcolloids and nanoparticles on cucumber early seedlings, *Sci. Total. Environ.*, 2022, **804**, 150233.

46 M. G. Park, Y. N. Kim, J. s. Lee, Y. J. Kim, S. Y. Kim, S. Choi, M. H. Yang, B. O. Kwon, J. R. Rho and E. J. Jeong, Variations in metabolites content and bioactivity to regulate biomarkers of benign prostatic hyperplasia according to the growth stages of Sida rhombifolia, *Arab. J. Chem.*, 2025, **18**, 106071.

47 S. Payamifar, M. Abdouss and A. P. Marjani-Arabian, The application of magnetic nanoparticles based β-cyclodextrin as recoverable catalyst in various organic transformations: An overview, *Arab. J. Chem.*, 2025, **18**, 106080.

48 S. Plokhovska, E. Fuente-González, E. Gutierrez-Albanchez, F. J. Gutierrez-Mañero and B. Ramos-Solano, AgNPs biosynthesized from Pseudomonas Z9.3 metabolites as antimicrobial agents against bacterial and fungal pathogens, *Front. Microbiol.*, 2025, **16**, 1565689.
49 A. M. M. Saeed, G. P. Cao, A. S. Al-Fatesh, S. B. Alreshaidan, N. Ali, M. S. Shehu and J. Y. Yan, Highly efficient platinum nano-particles decorated multi-walled carbon nanotubes (Pt/MWCNTs) catalyst for catalytic hydrogenation of styrene–butadiene–styrene (SBS)copolymer, *Arab. J. Chem.*, 2024, **17**, 105983.
50 S. L. Wang, Y. X. Zhang, H. Z. Liu and H. Xin, Phytotoxicity of copper oxide nanoparticles to metabolic activity in the roots of rice, *Acta. Sci. Circumstantiae*, 2014, **35**, 1968–1973.
51 C. Liu, Y. Yu, H. Liu and H. Xin, Effect of different copper oxide particles on cell division and related genes of soybean roots, *Plant. Physiol. Biochem.*, 2021, **163**, 205–214.
52 S. Khan, N. Akhtar, S. U. Rehman, S. Shujah, E. S. Rha and M. Jamil, Bacillus subtilis Synthesized Iron Oxide Nanoparticles ($Fe_3O_4$ NPs) Induced Metabolic and Anti-Oxidative Response in Rice (*Oryza sativa* L.) under Arsenic Stress, *Toxics*, 2022, **10**, 618.
53 A. Pitzschke, C. Forzani and H. Hirt, Reactive oxygen species signaling in plants, *Antioxid. Redox Signal*, 2006, **8**, 1757–1764.
54 P. Debnath, A. Mondal, K. Sen, D. Mishra and N. K. Mondal, Genotoxicity study of nano $Al_2O_3$, $TiO_2$ and ZnO along with UV-B exposure: An Allium cepa root tip assay, *Sci. Total. Environ.*, 2020, **713**, 136592.
55 L. R. R. Souza, L. E. Bernardes, M. F. S. Barbetta and M. A. M. S. Da Veiga, Iron oxide nanoparticle phytotoxicity to the aquatic plant Lemna minor: effect on reactive oxygen species (ROS) production and chlorophyll a/chlorophyll b ratio, *Environ. Sci. Pollut. Res.*, 2019, **26**, 24121–24131.
56 I. Moreno-Garrido, S. Pérez and J. Blasco, Toxicity of silver and gold nanoparticles on marine microalgae, *Mar. Environ. Res.*, 2015, **111**, 60–73.
57 R. Kaveh, Y. S. Li, S. Ranjbar, R. Tehrani, C. L. Brueck and B. V. Aken, Changes in arabidopsis thaliana gene expression in response to silver nanoparticles and silver ions, *Environ. Sci. Technol.*, 2013, **47**, 10637–10644.
58 E. K. Baghkheirati and J. G. Lee, Gene Expression, Protein Function and Pathways of *Arabidopsis thaliana* Responding to Silver Nanoparticles in Comparison to Silver Ions, Cold, Salt, Drought, and Heat, *Nanomaterials*, 2015, **5**, 436–467.
59 N. Amist, N. B. Singh, K. Yadav, S. C. Singh and J. K. Pandey, Comparative studies of$Al^{3+}$ ions and $Al_2O_3$ nanoparticles on growth and metabolism of cabbage seedlings, *J. Biotechnol.*, 2017, **254**, 1–8.
60 F. Yanik and F. Vardar, Toxic Effects of Aluminum Oxide ($Al_2O_3$) Nanoparticles on Root Growth and Development in *Triticum aestivum*, *Water Air Soil Poll.*, 2015, **226**, 296.
61 W. B. Musgrave, H. Yi, D. Kline, J. C. Cameron, J. Wignes, S. Dey, H. B. Pakrasi and J. M. Jez, Probing the origins of glutathione biosynthesis through biochemical analysis ofglutamate-cysteine ligase and glutathione synthetase from a model photosynthetic prokaryote, *Biochem. J.*, 2012, **450**, 63–72.
62 I. H. Estévez and M. R. Hernández, Plant glutathione S-transferases: An overview, *Plant Gene*, 2020, **23**, 100233.
63 J. H. Chen, H. W. Jiang, E. J. Hsieh, H. Y. Chen, C. T. Chien, H. L. Hsieh and T. P. Lin, Drought and salt stress tolerance of an *Arabidopsis* glutathione S-transferase U17 knockout mutant are attributed to the combined effect of glutathione and abscisic acid, *Plant. Physiol.*, 2011, **158**, 340–351.
64 B. Jha, A. Sharma and A. Mishra, Expression of SbGSTU (tau class glutathione S-transferase) gene isolated from Salicornia brachiata in tobacco for salt tolerance, *Mol. Biol. Rep.*, 2010, **38**, 4823–4832.
65 G. Diao, Y. Wang, C. Wang and C. Yang, Cloning and Functional Characterization of a Novel Glutathione S-Transferase Gene from *Limonium bicolor*, *Plant. Mol. Biol. Rep.*, 2010, **29**, 77–87.
66 J. Zhai, H. Li, S. Gao, H. Sun, C. Zhao, D. Yu, X. Lin, S. Cheng and J. Li, Corrigendum to "Palladium nanocubes-mediated Fenton catalysis combined with chloride ion-amplified electro-driven catalysis for dye degradation", *Arab. J. Chem.*, 2024, **18**, 106087.
67 A. Lanzinger, T. Frank, G. Reichenberger, M. Herz and K. H. Engel, Metabolite profiling of barley grain subjected to induced drought stress: responses of free amino acids in differently adapted cultivars, *J. Agr. Food. Chem.*, 2015, **63**, 4252–4261.
68 V. Zemanová, M. Pavlík, D. Pavlíková and P. Tlusto, The significance of methionine, histidine and tryptophan in plant responses and adaptation to cadmium stress, *Plant. Soil. Environ.*, 2014, **60**, 426–432.
69 L. B. Zoghlami, W. Djebali, Z. Abbes, H. Hediji, M. Maucourt, A. Moing, R. Brouquisse and W. Chaibi, Metabolitemodifications in Solanum lycopersicum roots and leaves under cadmium stress, *Afr. J. Biotechnol.*, 2011, **10**, 567–579.
70 J. Sun, L. Wang, S. Li, L. Yin, J. Huang and C. Chen, Toxicity of silver nanoparticles to *Arabidopsis*: Inhibition of root gravitropism by interfering with auxin pathway, *Environ. Toxicol. Chem.*, 2017, **36**, 2773–2780.
71 C. C. Kan, T. Y. Chung, H. Y. Wu, Y. A. Juo and M. H. Hsieh, Exogenous glutamate rapidly induces the expression of genes involved in metabolism and defense responses in rice roots, *BMC Genomics*, 2017, **18**, 186.
72 T. H. Kim, E. C. Kim, S. W. Kim, H. S. Lee and D. W. Choi, ExogenousGlutamate Inhibits the Root Growth and Increases the Glutamine Content in *Arabidopsis thaliana*, *J. Integr. Plant Biol.*, 2009, **53**, 45–51.
73 W. L. Pia, I. I. Ivanov, F. Sophie, G. Yinbo, R. Tony and F. Briang, Nitrogen Regulation of Root Branching, *Ann. Bot.*, 2006, **97**, 875–881.
74 C. M. Kinoan and H. Katas, Sustainable production and antibacterial efficacy of silver nanoparticles on cellulose nanofibers from mushroom waste, *RSC Adv.*, 2025, **15**, 19726–19740.

75 S. H. Lee, S. J. Ahn, Y. J. Im, K. Cho, G. C. Chung, B. H. Cho and O. Han, Differential impact of low temperature on fatty acid unsaturation and lipoxygenase activity in figleaf gourd and cucumber roots, *Biochem. Bioph. Res. Co.*, 2005, **330**, 1194–1198.

76 T. Wongsheree, S. Ketsa and W. G. Van Doorn, Technology, The relationship between chilling injury and membrane damage in lemon basil (*Ocimum* × *citriodourum*) leaves, *Postharvest Biol. Technol.*, 2009, **51**, 91–96.

77 G. H. Lim, R. Singhal, A. Kachroo and P. Kachroo, Fatty Acid- and Lipid-Mediated Signaling in Plant Defense, *Annu. Rev. Phytopathol.*, 2017, **55**, 505–536.

78 C. Maurel, L. Verdoucq, D. T. Luu and V. Santoni, Plant aquaporins: membrane channels with multiple integrated functions, *Annu. Rev. Plant Biol.*, 2008, **59**, 595–624.

79 D. Bartels and R. Sunkar, Drought and Salt Tolerance in Plants, *Crit. Rev. Plant. Sci.*, 2005, **1**, 24.

80 M. S. Kim, S. M. Cho, E. Y. Kang, Y. J. Im, H. Hwangbo, Y. C. Kim, C. M. Ryu, K. Y. Yang, G. C. Chung and B. H. Cho, Galactinol Is a Signaling Component of the Induced Systemic Resistance Caused by Pseudomonas chlororaphis O6 Root Colonization, *Mol.Plant. Microbe. In.*, 2008, **21**, 1643.

81 H. Scheller and P. Ulvskov, Hemicelluloses, *Annu. Rev. Plant Biol.*, 2010, **61**, 263–289.

82 R. Franke, R. Höfer, I. Briesen, M. Emsermann, N. Efremova, A. Yephremov and L. Schreiber, The DAISY gene from *Arabidopsis* encodes a fatty acid elongase condensing enzyme involved in the biosynthesis of aliphatic suberin in roots and the chalaza-micropyle region of seeds, *Plant J.*, 2009, **57**, 80–95.

83 V. Shukla and M. Barberon, Building and breaking of a barrier: Suberinplasticity and function in the endodermis, *Curr. Opin. Plant Biol.*, 2021, **64**, 102153.

84 P. E. Kolattukudy, Polyesters in Higher Plants, *Biopolyesters*, 2001, **71**, 1–49.

85 M. Pollard, F. Beisson, Y. H. Li and J. B. Ohlrogge, Building lipid barriers: biosynthesis of cutin and suberin, *Trends. Plant. Sci.*, 2008, **13**, 236–246.

86 R. Höfer, I. Briesen, M. Beck, F. Pinot, L. Schreiber and R. Franke, The Arabidopsis cytochromeP450 CYP86A1 encodes a fatty acid ω-hydroxylase involved in suberin monomer biosynthesis, *J. Exp. Bot.*, 2008, **59**, 2347–2360.

87 N. D. G. De Silva, J. Murmu, D. Chabot, K. Hubbard, P. Ryser, I. Molina and O. Rowland, Root Suberin Plays Important Roles in Reducing Water Loss and Sodium Uptake in Arabidopsis thaliana, *Metabolites*, 2021, **11**, 735.

88 M. Soler, O. Serra, M. Molinas, G. Huguet, S. Fluch and M. Figueras, A Genomic Approach to Suberin Biosynthesis and Cork Differentiation, *Plant. Physiol.*, 2007, **144**, 419–431.

89 R. Höfer, I. Briesen, M. Beck, F. Pinot, L. Schreiber and R. Franke, The *Arabidopsis* cytochrome P450 CYP86A1 encodes a fatty acid omega-hydroxylase involved in suberin monomer biosynthesis, *J. Exp. Bot.*, 2008, **59**, 2347–2360.

90 W. Zeng, Z. Sun, Y. Liu, Q. Zhou, Y. Zhang, Y. Qiu, H. Fu, H. Zou, H. Pu and W. Xue, Design and research of new virulence factor inhibitors for plant bacterial disease control, *Arab. J. Chem.*, 2024, **17**, 106042.

91 C. D. Albright, C. B. Friedrich, E. C. Brown, M. H. Mar and S. H. Zeisel, Maternal dietary choline availability alters mitosis, apoptosis and the localization of TOAD-64 protein in the developing fetal rat septum, *Dev. Brain. Res.*, 1999, **115**, 123–129.

92 E. A. Alabdullkarem and J. Khan, Dual-function g-$C_3N_4$ anchored Cu–ZnS hybrid nanostructures for sustainable energy storage and environmental remediation, *RSC Adv.*, 2025, **15**, 23801–23818.

93 R. E. Häusler, F. Ludewig and S. Krueger, Amino acids–A life between metabolism and signaling, *Plant Sci.*, 2014, **229**, 225–237.

94 D. Wipf, U. Ludewig, M. Tegeder, D. Rentsch, W. Koch and W. B. Frommer, Conservation of amino acid transporters in fungi, plants and animals, *Trends. Biochem. Sci.*, 2002, **27**, 139–147.

95 G. S. Liu, Y. Y. Ji, N. H. Bhuiyan, G. Pilot, G. Selvaraj, J. Zou and Y. D. Wei, Amino acid homeostasis modulates salicylic acid-associated redox status and defense responses in *Arabidopsis*, *Plant Cell*, 2010, **22**, 3845–3863.

96 S. S. Sharma and K. J. Dietz, The significance of amino acids and amino acid-derived molecules in plant responses and adaptation to heavy metal stress, *J. Exp. Bot.*, 2006, **57**, 711–726.

97 B. Das, A. Padhiary, S. Behera, S. Mishra, M. Jena, S. Swain and S. Rout, Biochemical Changes in Some Rice Varieties in Response to Waterlogged and Submerged Conditions, *Energy. Environ. Sci.*, 2017, **5**, 972–978.

98 A. E. Moukhtari, C. Cabassa-Hourton, M. Farissi and A. Savouré, How DoesProline Treatment Promote Salt Stress Tolerance During Crop Plant Development, *Front. Plant. Sci.*, 2020, **11**, 1127.

99 A. M. Kinnersley and F. Turano, Gamma Aminobutyric Acid (GABA) and Plant Responses to Stress, *Crit. Rev. Plant Sci.*, 2000, **19**, 479–509.

100 C. T. Chen and R. D. Slocum, Biochemistry, Expression and functional analysis of aspartate transcarbamoylase and role of *de novo* pyrimidine synthesis in regulation of growth and development in Arabidopsis, *Plant Physiol. Biochem.*, 2008, **46**, 150–159.

101 R. Katahira and H. Ashihara, Dual function of pyrimidine metabolism in potato(Solanum tuberosum) plants: pyrimidine salvage and supply of β-alanine to pantothenic acid synthesis, *Physiol. Plantarum*, 2006, **127**, 38–43.

102 C. Stasolla, R. Katahira, T. A. Thorpe and H. Ashihara, Purine and pyrimidine nucleotide metabolism in higher plants, *J. Plant Physiol.*, 2003, **160**, 1271–1295.